Proceedings of the 2006 IASME/WSEAS International Conference on Energy & Environmental Systems, Chalkida, Greece, May 8-10, 2006 (pp95-102)

Experimental and Theoretical Investigation of a Capillary Pumped Loop

D. P. MARGARIS[*], Z. G. DIAMANTIS[†], D. I. PHOTEINOS[†], D. T. TSAHALIS[†]
[*] Fluid Mechanics Laboratory (FML/UoP)
Department of Mechanical Engineering and Aeronautics
University of Patras, 26500 Patras, GREECE

[†] Laboratory of Fluid Mechanics and Energy (LFME)
Department of Chemical Engineering
University of Patras, P.O. BOX 1400, 26500 Patras, GREECE

Abstract: - The objective of this paper is to present a theoretical investigation of the operational characteristics on a small-scale Capillary Pump Loop (CPL). A typical design of a CPL is composed of a capillary evaporator, a condenser, a two-phase reservoir, and liquid and vapor lines. The capillary evaporator generates the required pressure pumping for moving the working fluid from the condenser to the evaporator section. The fundamental principles of the proposed modeling are: The overall pressure drop in the loop must be less than the maximum capillary pressure in order to ensure that the system will operate continuously. The major components of the CPL pressure drop are related to the flow in the wick structure, condenser, vapor and liquid lines. The wick structure present in the evaporator causes flow restriction that affects the CPL performance, which is dependent on the wick permeability, a property of the porous material that describes its ability to transport the liquid under an applied pressure gradient. An experimental lab-scale installation is used for the validation of the theoretical analysis. The results showed that the proposed CPL modeling is able to describe very well the CPL performance.

Keywords: - Capillary pump, CPL, heat pipes.

1 Introduction

Capillary pumping two-phase loops have been continuously investigated for electronic cooling systems, satellite thermal control and other space applications. Most tests were performed in capillary evaporators using plastic or metallic porous wick as capillary structure and anhydrous ammonia as the working fluid.

A Capillary Pump Loop (CPL) is designed for operation as a two-phase heat transfer device in passive mode, without need of any mechanical pump for driving the working fluid from a low temperature sink to high temperature source. Although earth-based applications of the CPL have been proposed, it is especially well suited for thermal management in spacecraft, where gravity and hence its potentially deleterious effects on the CPL's operation are absent. The CPL uses capillary action for fluid transport and contains no moving parts. Multiple evaporators and condensers can be added at different locations in a CPL, allowing the use of a single loop to reject heat from multiple sources to multiple sinks, possibly at different temperatures. In contrast to the heat pipe, wicks are absent in most of the transport section of the CPL. Instead, liquid and vapor flow trough smooth walled tubing, thereby reducing the frictional pressure losses and increasing the maximum potential fluid flow and heat transfer rates.

A typical design of a CPL (Fig. 1) is composed of a capillary evaporator (responsible for generating capillary forces that drive the working fluid), a condenser, a two-phase reservoir (to control the loop saturation pressure), and liquid and vapor lines. The capillary forces are generated by the capillary evaporator, which acquires heat and transfers it to the working fluid. Formation of vapor is responsible for the displacement of the liquid in the lines towards the condenser during the start up. The two-phase reservoir is used to set the operation temperature at which the entire loop will operate.

The CPL works without moving parts and very little power consumption. The fluid must be used in its pure state without contaminants, which enables its use in microgravity. It passively promotes the thermal control, allowing fine control on the operating temperature of components.

CPL development began in the 1960s but received special attention in the late 1970s. At this time, CPL began to be intensively investigated, proving to be operationally reliable for thermal control and able to transport heat over long distances with minor temperature difference. Excellent reviews of the development history and theory of operation are available in the literature [1, 2]. In recent years, numerous CPLs have been fabricated and ground-tested, several have been tested in flight experiments and designs have been selected for use on a few spacecraft missions [3]. Nevertheless, issues relating to the CPL's reliability and robustness have limited its acceptance and implementation, and have been the primary focus in recent years [4-7].

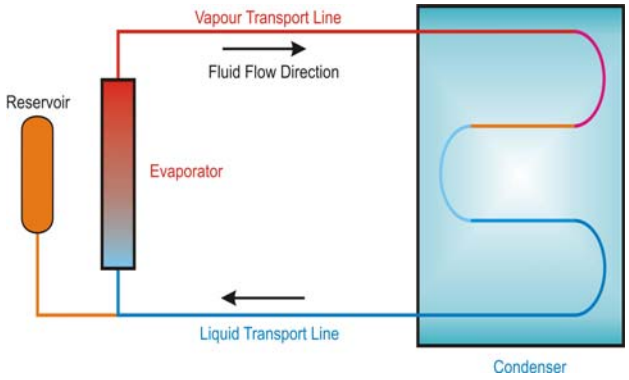

Fig. 1. **S**chematic diagram of the CPL.

One problem which has plagued CPLs in both ground and flight tests is the difficulty in starting the evaporators. Typically, after a CPL successfully starts and enters into a steady operation mode it performs quite well and the operation is fairly predictable. However, before steady state operation can occur, a series of transient events, collectively referred to as the start-up, must take place where the thermophysical state of fluid through much of the loop changes quite dramatically. During the start-up, the locations occupied by liquid and vapor transiently shift to those corresponding to steady state operation. This repositioning of liquid and vapor occurs through the combined processes of vaporization, condensation, and multi-phase fluid flow through various portions of the loop.

In theory, vapor should form only in the vapor grooves of an evaporator. Vapor presence in the liquid core has been found to fully or partially block liquid flow to the wick, which may lead eventually to deprime – the loss of capillary pumping action – of an evaporator [8, 9]. Also, vapor presence in the evaporator core has been to influence pressure oscillations in the CPL [10].

The two-phase reservoir has to be heated, prior to the start-up of a CPL, so that the operation temperature can be set. The entire loop will then operate at this temperature with slight variations owing to some superheat or subcooling. Upon setting an operating temperature in the reservoir, the internal pressure will raise which will fill the entire loop with liquid, causing the so-called pressure priming. When the loop is filled with liquid, the CPL is ready to start operating. Then, heat is applied to the capillary evaporator and as its temperature rises, only sensible heat is transferred to the working fluid. When the evaporator temperature reaches the same temperature as the reservoir, latent heat is transferred to the working fluid starting the evaporation process. A meniscus is formed at the liquid-vapor interface, which is responsible for developing the capillary pressure that will drive the working fluid. Vapor is displaced from the evaporator, which causes the displacement of the liquid in the channels allowing the vapor to reach the condenser. In the condenser, heat is removed and liquid will also present some subcooling. At the start-up, the excess of liquid present in the channels is displaced by the vapor back to the reservoir, which equalizes the right amount of working fluid for a given heat load. With such particularities, the CPL has been used to transfer heat over long distances with small pressure drops over the entire loop allowing its use in large systems. CPLs have been tested over different configurations, and it is known to transport up to 5000 W when capillary evaporators are used [11]. Without moving parts and because a CPL acts as a thermal diode, the working fluid cannot flow from the condenser to the evaporator by the vapor line.

Different materials have been used as porous wick such as sintered nickel, stainless steel, titanium and ultra-high molecular weight polyethylene [12-14]. As the generation of capillary forces is dependent on the working fluid surface tension and wick pore size, CPLs have been investigated using methanol, acetone and anhydrous ammonia as working fluids. Several investigations have been performed towards the achievement of sintered nickel components with fine pore sizes [15, 16].

Nowadays, there are efforts to extend the application of capillary pumps loops to commercial and industrial systems. Very few investigations have been conducted towards the use of small size capillary evaporator in order to manufacture a more compact CPL. Investigators [17] have reported that small evaporators have a tendency of depriming more easily probably due to an insufficient subcooled liquid supply to the porous wick.

The objective of this paper is to present a theoretical investigation of the operational characteristics on a small-scale CPL. An experimental lab-scale installation, described analytically in [18] and the modified configuration in [19], is used for the validation of the theoretical analysis. The results showed that the proposed CPL modeling is able to describe very well the CPL performance.

2. EXPERIMENTAL SETUP AND PROCEDURES

2.1 Experimental Setup

Initially the experimental setup consisted of a 70 cm long sintered material filled pipe and the liquid/vapour sections of the setup were approximately 7 m long. However, after some experience had been gained in starting up the system, it was decided to try a smaller/shorter configuration. This led to a reduction of the experimental setup to about one-third its initial size, i.e., liquid/vapour sections about 2.5 m long.

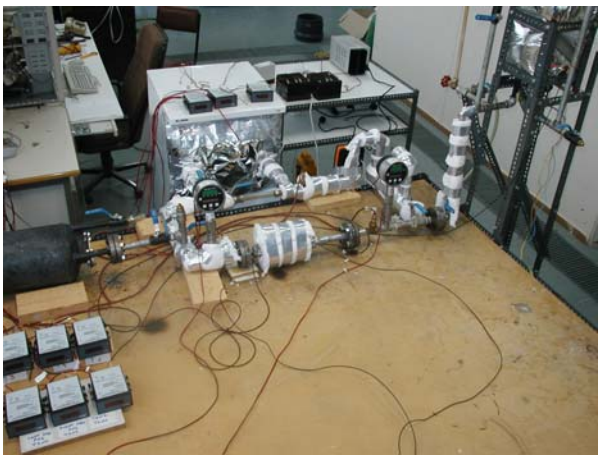

Fig. 2. Configuration of the experimental setup with 3 - 2cm sintered material filled pipe.

Fig. 3. Bundle of 3 - 2cm long sintered material filled pipe.

Furthermore, in order to increase the flowrate, multiple, parallel evaporator configurations were tried in addition to the single sintered material filled pipe. Specifically, three 15cm-long evaporator configurations, consisting of 1, 3 and 7 sintered material filled pipes, respectively, bundled together were built.

After performing tests with different experimental setups the configuration of sintered material filled pipes that is currently being used is 2-cm long (Fig. 2) and consisting of a bundle of 3 pipes (Fig. 3).

The diagram of the experimental setup designed and developed by LFME is given in fig. 4. The description of its main components follows the numbering shown in figure 4:

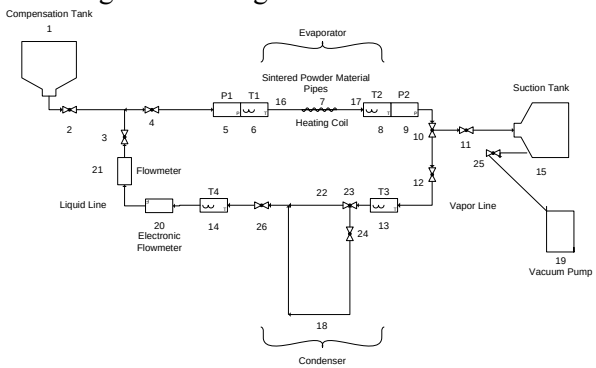

Fig. 4. Diagram of the experimental setup indicating the position of major components.

#1. 10 liter compensation tank. #2, 3, 10, 11, 12, 23 and 24 Ball valves. #4. Filter. #5 and 9. Kobold MAN-SF26 pressure gauges, P1 and P2, respectively. #6, 8, 13 and 14 Kobold TSA1105 Pt100 thermocouples, T1, T2, T3 and T4, respectively. #7. The sintered material filled pipes and the heating coil. #15. 10 liter suction tank. #16 and 17. Kobold TWA R6A 03012P thermocouples

placed on the surface, on each side of the sintered material filled pipe. #18. Kobold TWA R6A 03012 placed on the surface of the pipe. #19. DVP LA 12 vacuum pump. #20 The electronic flowmeter type Kobold KMI-1209HN2A40. #21. Kobold KDF-1125-NV flowmeter. #26 One way valve that allows flow only in the direction of the liquid line and not in the direction of the vapour line.

The pipes loop is made of ½ inch stainless steel pipe which can withstand pressures up to 12 bars. The majority of the loop is insulated by means of a special ceramic material very similar to that used in fireproof blankets. The material is used to assure that the system is not affected by external fluctuations of temperature. The same material is also used around the heating coil and can withstand temperatures up to 1350 ^{0}C without igniting.

All pressure and temperature sensors are connected to a PC-based data acquisition system for continuous monitoring on the PC monitor and simultaneous digitization and storing. The software is based on the well known software package Labview (version 6i). The PC was equipped with a National Instruments PCI-MIO-16E-4 data acquisition card.

2.2 Experimental procedure and results

Initially, the compensation tank is filled with distilled water in order to avoid having blocking phenomena later on in the sintered powder material due the presence of various unwanted minerals and salts in the water when its temperature is brought to the desired level. During the heating of the water in the compensation tank, the vacuum pump is turned on until the desired level of vacuum has been achieved in the pipe system and the vacuum tank.

The bundle of triple 2 cm long sintered material filled pipes achieved the steadiest periodical flow ever observed. The flowrates did not exceed 6 lt/hr, however for the whole time that the system was running under steady state temperature conditions there was a periodical flow in the system in the range of 2 to 4 lt/hr

The following figure (Fig. 5) is a compilation of the measurements obtained from one of the triple pipe experiments that were performed. Before presenting these results, it should be noted that the setup under examination was not fully insulated during the experiment and that the average heat provided by the heating coil was 300 Watt. Furthermore, the flow values are average values for a specific series of time steps, this means that at no time was steady flow observed in the system, as it will be seen in the graph, but only “spikes” of flow were observed.

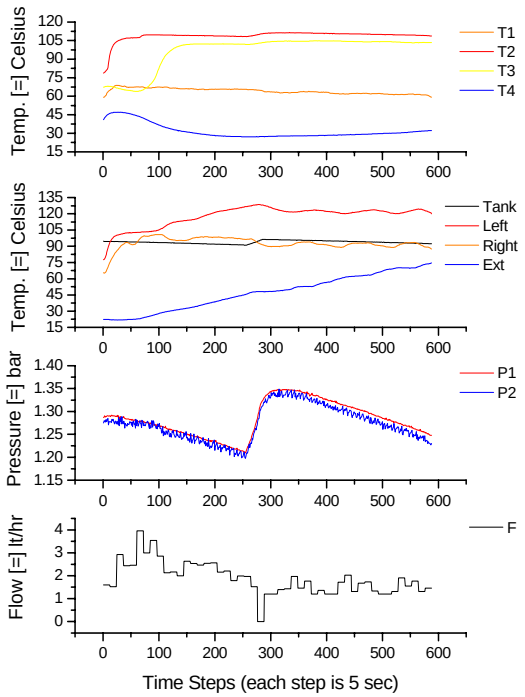

Fig. 5. Compilation of the measurements obtained from one of the triple pipe experiments that were performed.

In the graph we notice that the T2 and T3 temperatures during the whole time of periodic flow, are very close and at about 100 ^{0}C, which means that steam is constantly being created in the vapor side of the setup. In the beginning, before the stabilization of temperatures T2 and T3 we notice that large flowrates are observed, but they are rather more like spikes and do not have a periodic nature. When temperatures stabilize, the periodic flowrate observed is between 1 and 2 lt/hr. On the liquid side of the setup, temperatures are also constant, T1 and T4. For T4 we notice that it starts a bit high, around 45^{0}C and then it drops to an average of 30^{0}C. This is due to the fact that the refrigerator was not used from the beginning of the experiment for the cooling of the vapor line, but only after the temperature in T3 exceeded 75^{0}C. At the same time, on the exterior of the setup we notice that the temperatures on the Left and Right side of the sintered material filled pipes are quite stable and there is an average difference of 30^{0}C. Concerning the pressures, we notice that P1 is more stable than P2, however they both have a similar response during the whole time. The continuous changes in P2 show that steam is being created

continuously during the whole time of the experiment. It can also been seen that at all times P1 is slightly greater than P2. The large step that is seen at Time Step 250 can be explained by the fact that at that certain point the heater in the compensation tank turned on and the temperature in the tank rose, as it can be seen by the Tank temperature curve, thus leading to a total rise in pressure of the whole system of about 0.15 bar.

Similar results have been obtained for various experimental runs, thus showing that the sintered material filled pipe is able to create a certain amount of flow.

3 Modelling of a CPL

The CPL design is related to the maximum capillary pressure that can be developed by the wick structure and working fluid. The overall pressure drop in the loop must be less than the maximum capillary pressure in order to ensure that the system will operate continuously. Thus the driving pressure difference Δp_{eff} is given by:

$$\Delta p_{eff} = \Delta p_{c,max} + \Delta p_b - \Delta p_{total} \quad (1)$$

where $\Delta p_{c,max}$ is the pressure drop due to maximum capillary force, Δp_b is the pressure drop due to buoyancy force effect, and Δp_{total} is the total pressure drop in the overall loop.

The pressure drop due to maximum capillary force is given by:

$$\Delta p_{c,max} = \frac{2\sigma_L}{r_c} \quad (2)$$

with σ_L the surface tension and r_c the radius. The pressure drop due to buoyancy force effect is:

$$\Delta p_b = (\rho_\lambda - \rho_v) g h \quad (3)$$

with ρ the density of liquid and vapor respectively.

The major components of the CPL pressure drop are related to the flow in the evaporator (wick structure), condenser, vapor and the liquid lines. Thus the total pressure drop in the overall loop is given by

$$\Delta p_{total} = \Delta p_w + \Delta p_\lambda + \Delta p_v + \Delta p_c + \Delta p_g \quad (4)$$

The pressure drop in the evaporator due to liquid flowing through the porous media (based on the Darcy's law) may be written as:

$$\Delta p_w = \frac{\mu_\lambda \lambda_w \dot{m}}{\rho_\lambda K_w A_w} \quad (5)$$

where λ_w the length, A_w the surface, and K_w the permeability of the porous media (wick) and $\dot{m}$ the mass flow rate.

The pressure drop in the condenser is related to the mass velocity G of the liquid, the velocity of the liquid u_l and the velocity of the vapor u_v through the equation

$$\Delta p_c = \frac{G_\lambda}{g_c}(u_v - u_\lambda) \quad (6)$$

where g_c is the gravitational conversion constant.

The mass velocity G_l and the liquid velocity u_l are given by the equations

$$G_\lambda = \frac{4\rho_\lambda Q_\lambda}{\pi d_{c,h}^2} \quad \text{and} \quad u_\lambda = \frac{4Q_\lambda}{\pi d_{c,h}^2} \quad (7)$$

and the flow rate of the liquid Q_l and the vapour Q_v are related with the equation

$$Q_v = \frac{\rho_\lambda}{\rho_v} Q_\lambda \quad (8)$$

where ρ_l is the density of the liquid and ρ_v is the density of the vapor.

Substituting Eq.(7) and (8) into Eq.(6) it is obtained that

$$\Delta p_c = \frac{16}{g_c \pi^2 d_{c,h}^4}\left(\frac{\rho_\lambda}{\rho_v} - 1\right)\rho_\lambda Q_\lambda^2 \quad (9)$$

The pressure drop due to liquid flowing through the liquid head line and the vapor head line is given by

$$\Delta p_\lambda = f \frac{\lambda_\lambda}{d_{\lambda,h}} \frac{\rho_\lambda u_\lambda^2}{2} \qquad \Delta p_v = f \frac{\lambda_v}{d_{v,h}} \frac{\rho_v u_v^2}{2} \quad (10)$$

where λ the length and d_{lh} the hydraulic diameter of the liquid or the vapor head line and f the friction factor dependent on the Reynolds number of each phase, f(Re).

And finally the pressure drop due to gravitational head effect is given simply by the equation

$$\Delta p_g = \rho_\lambda g h \qquad (11)$$

Usually the flow is in the laminar region, Re<2300, so f=64/Re, and by substitution into Eqs (10) we get

$$\Delta p_\lambda = \frac{128\mu_\lambda\lambda_\lambda}{\pi d_{\lambda,h}^4} Q_\lambda \qquad \Delta p_v = \frac{128\mu_v\lambda_v\rho_\lambda}{\pi d_{v,\lambda}^4\rho_v} Q_\lambda \qquad (12)$$

By combining Eqs (5), (9), (11) and (12) it is obtained

$$\Delta p_{total} = \frac{\mu_\lambda\lambda_w \dot{m}}{\rho_\lambda K_w A_w} + \frac{16}{g_c\pi^2 d_{c,h}^4}\left(\frac{\rho_\lambda}{\rho_v}-1\right)\rho_\lambda Q_\lambda^2 + \frac{128\mu_\lambda\lambda_\lambda}{\pi d_{\lambda,h}^4} Q_\lambda + \frac{128\mu_v\lambda_v\rho_\lambda}{\pi d_{v,\lambda}^4\rho_v} Q_\lambda + \rho_\lambda g h \qquad (13)$$

Eq.(13) gives the total pressure drop Δp_{total} in the loop from parameters which are either directly measurable (pipe length and diameter, flow rate) or material properties which can be found in the bibliography (viscosity of the fluids).

By means of the relation between fluid velocity, mass flow rate, input heat flux of the evaporator, Q_e, and enthalpy, $h_{l,v}$, it is possible to couple fluid dynamics with thermodynamics magnitudes, [20]. As a result the maximum power that can be removed by the natural convection for a given loop configuration is given by

$$Q_e = \left(2\frac{\sigma_L}{r_c} - \rho_\lambda g h + (\rho_\lambda - \rho_v) g h\right) \Bigg/ \left(\frac{\mu_\lambda\lambda_w}{\rho_\lambda K_w A_w h_{\lambda,v}} + \frac{16 Q_\lambda}{g_c\pi^2 d_{c,h}^4 h_{\lambda,v}}\left(\frac{\rho_\lambda}{\rho_v}-1\right) + C_1\frac{\mu_\lambda\lambda_\lambda}{\rho_\lambda d_{\lambda,h}^4 h_{\lambda,v}} + C_2\frac{\mu_v\lambda_v}{\rho_v d_{v,h}^4 h_{\lambda,v}}\right) \qquad (14)$$

From the above equation the maximum remove power of the capillary loop can be obtained.

4 Results and discussion

The experimental lab-scale installation, presented above and more analytical in [19], is used for the validation of the theoretical analysis. The wick thickness is $20\text{x}10^{-3}$ m, the transversal area is $3\text{x}1.131\text{x}10^{-4}$ m^2, pore radius is $3.17\text{x}10^{-5}$ m and its permeability $1.43\text{x}10^{-11}$ m^2. The length of the liquid line is 3.67 m, the length of the vapor line is 3.05 m and the diameter of the loop is ½ inches (0.0127 m). The properties of the liquid are those for 20 °C (density ρ_l = 998.2 kg/m^3, viscosity μ_l = $100.2\text{x}10^{-5}$ kg/ms, and surface tension σ = $71.97\text{x}10^{-3}$ N/m) and of the vapor are those for 100 °C (density ρ_v = 0.595 kg/m^3 and viscosity μ_v = $1.206\text{x}10^{-5}$ kg/ms).

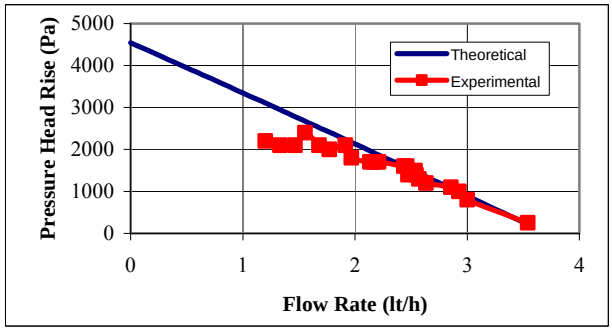

Fig. 6. Comparison between theoretical and experimental results of the pressure head rise vs. flow rate.

The results show that the above proposed CPL modeling is able to describe well the CPL performance. A sample of the comparison diagram between theoretical and experimental results for the pressure head rise vs. flow rate is given in Fig. 6. It is obvious that for higher flow rates there is a very good agreement between theoretical and experimental results. For flow rates lower than 1.5 lt/h there is a disagreement due to the unsteady character of the flow at the start-up period. As the time passes the temperatures are stabilized and the capillary pump loop operates steadily.

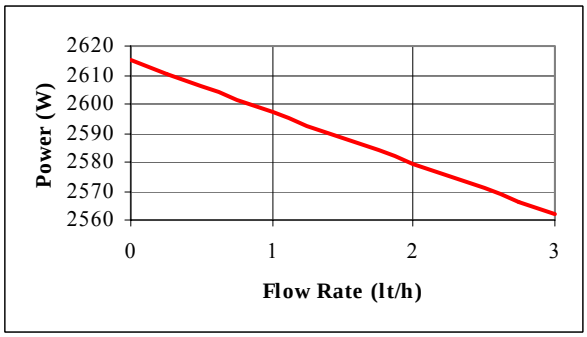

Fig. 7. The maximum remove power from the capillary pump loop as a function of the liquid flow rate.

Fig. 7 shows the maximum power that can be removed from the capillary pump loop as a function of the liquid flow rate. For the experimental installation and the conditions mentioned above, derives from Fig. 7 that the maximum power for liquid flow rate 1 lt/h is equal

to 2598 W, for 2 lt/h is 2589 W, and for 3 lt/h is 2562 W.

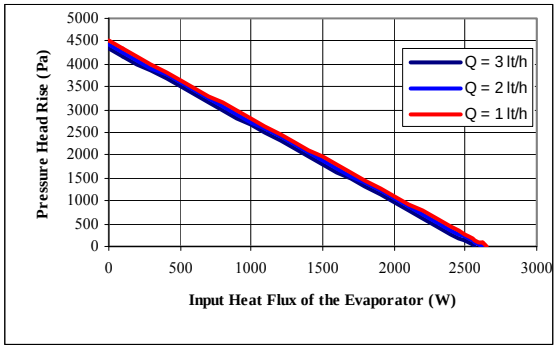

Fig. 8. Pressure head rise as a function of the input heat flux of the evaporator for different liquid flow rate.

The pressure head rise versus input heat flux of the evaporator is shown in Fig. 8 for different flow rates. Input heat flux of the evaporator affects very much the pressure head rise (or effective pressure drop). The function is linear and the liquid flow rate does not play significant role. Another result from this figure is that the maximum input heat flux of the evaporator or the maximum power is between 2560 and 2590 W which is the same result derived from Fig. 7. The conclusion is that the liquid flow rate does not affect very much the maximum power that can be removed from the capillary pump loop and as a result we may use a round value of 2600 W independent of the liquid flow rate. Applying the developed modeling to any installation with known geometry and flow conditions, it is possible to estimate the maximum power that can be removed by the capillary pump loop.

Pressure head rise as a function of the porous media surface is given in Fig. 9 for different liquid flow rates. The main result is that for any liquid flow rate there is a minimum value of the porous media surface necessary to start the flow. As it is clear, as higher the flow rates as larger the necessary surface for the loop operation. Another result is that as the porous media (or wick) surface increases, for a specific flow rate, the pressure head rise increases very much and then tends asymptotically to a constant value. The same behavior may be seen for the pressure head rise as a function of the permeability of the wick, which means that these parameters affect very much the operation of a capillary pump loop.

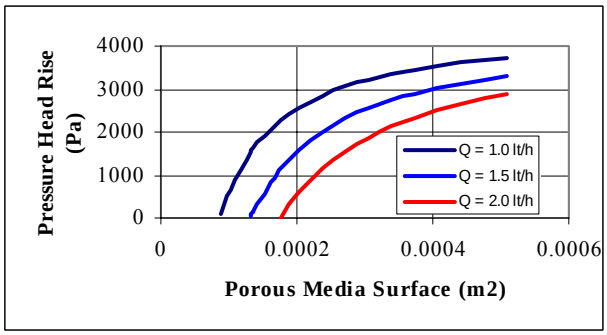

Fig. 9. Pressure head rise as a function of the porous media surface for different liquid flow rate.

5 Conclusions

A mathematical model was developed for the theoretical investigation of the operational characteristics on a small-scale Capillary Pump Loop (CPL). An experimental lab-scale installation was used for the validation of the theoretical analysis.

From the comparison diagram between theoretical and experimental results for the pressure head rise vs. flow rate, it is obvious that for higher flow rates there is a very good agreement between theoretical and experimental results. For lower flow rates there is a disagreement due to the unsteady character of the flow at the start-up period. As the time passes the temperatures are stabilized and the capillary pump loop operates steadily.

The liquid flow rate does not affect very much the maximum power that can be removed from the capillary pump loop and thus, for any installation with known geometry and flow conditions, it is possible to estimate a round value of the maximum power independent of the liquid flow rate.

The major components of the CPL pressure drop are related to the flow in the wick structure, vapor and the liquid lines. The results showed that the proposed CPL modeling is able to describe very well the CPL performance.

Acknowledgements

The work presented in this paper supported by the European Commission and performed under the framework of the FP5 project entitled “A Novel Tri-Generation Electro-gas-dynamic Converter System (TRI-GEN EGD)”, Contract Number ENK6-CT-2002-00686.

References

[1] Cullimore, B.A. (1993), "Capillary pumped loop application guide", SAE Paper 932156.

[2] Ku, J. (1993), "Overview of capillary pumped loop technology", *HTD- Vol. 236, in: Proceedings of the 29th National Heat Transfer Conference, Atlanta, GA, USA*, pp.1-17.

[3] Ku, J. (1997), "Recent advances in capillary pumped loop technology", AIAA Paper 97-3870.

[4] Hoang, T.T., Ku, J. (1995), "Theory of hydrodynamic stability for capillary pumped loops", *HTD-Vol. 307, in: Proceedings of the 1995 National Heat Transfer Conference, Portland, OR, USA,* Vol. 5, pp.33-40.

[5] Hoang, T., Ku, J., (1996), "Hydrodynamic aspects of capillary pumped loops", SAE Paper 961435.

[6] Hoang, T., (1997), "Development of an advanced capillary pumped loop", SAE Paper 972325.

[7] Kim, J.H., Cheung, K., Butler, D., Ku, J., Haught, E., Kroliczek, E.J., Cullimore, B., Baumann, J., (1997), "The capillary pumped loop III (CAPL III) flight demonstration description and status", *Proceedings of the Space Technology and Applications International Forum, Albuquerque, NM, USA,* pp. 623-628.

[8] Cullimore, B.A., (1991), "Start-up transients in capillary pumped loops", AIAA Paper 91-1374.

[9] Ku, J., (1995), "Start-up issues of capillary pumped loops", Advances in Heat Pipe Science and Technology, in: *Proceedings of the 9th International Heat Pipe Conference, Albuquerque, NM*, USA, pp. 994-1001.

[10] Ku, J., Hoang T., Nguyen, T., Yun, S., (1996), "Performance tests of CAPL 2 starter pump cold plates", AIAA Paper 96-1837.

[11] Grenier, H., Feuillatre, M., Maciaszek, T., Hustaix, H., (1995), "Development and test results of a 5 kW ammonia capillary pumped loop", *Proceedings of the 25th International Conference on Environmental Systems, San Diego, CA, USA,* paper 951505.

[12] Gerhart, C., Gluck, D., (1999), "Summary of operating characteristics of a dual compensation chamber loop heat pipe in gravity" *11th International Heat Pipe Conference, Tokyo, Japan.*

[13] Mulholland, G., Gerhart, C., Gluck, D., Stanley, S., (1999), "Comparison between analytical predictions and experimental data for loop heat pipes", *Space Technology and Applications International Forum, Albuquerque, NM, USA,* pp. 805-810.

[14] Ku, J., Ottenstein, L., Cheung, K., Hoang, T., Yun, S., (1998), "Ground tests of a capillary pumped loop (CALP 3) flight experiment", Proceedings of the 28th International Conference on Environmental Systems, Danvers, MS, USA, paper 981812.

[15] Reimbrecht, E.G., Fredel, M.C., Bazzo, E., Pereira, F.M., (1999), "Manufacturing and micro-structural characterization of sintered nickel wicks for capillary pumps", Mater. Res. 2 (3), pp. 225-229.

[16] Reimbrecht, E.G., Philippi, P.C., Bazzo, E., (2001), "Wick characterization by image analysis", Proceedings of the 30th ICES-International Conference on Environmental Systems, paper 2238.

[17] Delil, A.A.M., DuBois, M., Supper, W., (1997), "The European two-phase experiments TPX I & II", 10th International Heat Pipe Conference, Stuttgart, Germany.

[18] Diamantis, Z. G., Photeinos, D.I. and Tsahalis, D.T., "Investigation of the performance of heat pipes used as capillary pumps", SET 3 - *3rd International Conference on Sustainable Energy Technologies, Nottingham, UK, 28-30 June 2004*.

[19] Diamantis, Z. G., Photeinos, D.I., Margaris, D. P. and Tsahalis, D.T., "Development of an experimental setup to investigate the performance of heat pipes as capillary pumps", *1st Int. Conf. on Experiments/ Process/System/Modelling/Simulation/Optimization, 1st IC-EpsMsO, Athens, Greece, 6-9 July, 2005.*

[20] Margaris, D.P., Diamantis, Z.G., Photeinos, D.I., Tsahalis, D.T., "Modelling Of The Flow Behaviour In A Capillary Pumped Loop", *1st International Conference on "Experiments/ Process / System Modelling/ Simulation / Optimization", 1st EpSMsO, Athens, 6-9 July, 2005.*